# Characteristics of Wet and Dry Spells over the Pacific Side of Central America during the Rainy Season

Malaquías Peña

*Department of Meteorology, University of Maryland at College Park, College Park, Maryland*

Michael W. Douglas

*National Severe Storms Laboratory, Norman, Oklahoma*

## ABSTRACT

This paper describes the mean atmospheric conditions associated with synoptic-scale rainfall fluctuations over Central America during the rainy season. The study is based on composites of wet and dry spells; these composites are generated from six years (1990–94 and 1997) of daily rainfall observations from select Central American stations, one year (1997) of upper-air wind data from an enhanced sounding network over the region, National Center for Environmental Prediction (NCEP) reanalysis data, and outgoing longwave radiation (OLR) data. Wet spells, defined as days when 75% or more of the stations along the Pacific side of Nicaragua, Costa Rica, and Panama reported rainfall, are associated with weaker trade winds over the Caribbean and stronger cross-equatorial flow northward over the eastern Pacific. During wet spells the intensity of eastern Pacific cross-equatorial flow exceeds by several meters per second the seasonal mean in the lower and middle troposphere, and is strongest and deepest one day before the wettest day. Dry spells, defined as the days when 35% or less of these stations reported rainfall, are associated with stronger trade winds over Central America and weaker and shallower cross-equatorial flow. The basic flow patterns seen in the observation-based composites agree well with similar composites produced using reanalysis data, except that the observations show stronger cross-equatorial flow in the lower-mid troposphere over the eastern Pacific. OLR data shows that convective cloudiness anomalies associated with the wet and dry spells extend westward from Central America into the eastern tropical Pacific.

## 1. Introduction

Most of the major population centers in Central America are located on the Pacific side of the isthmus, in the lee of topography with respect to the prevailing trade wind flow (Fig. 1). Here, a well-defined annual cycle of precipitation is characterized by a rainy season from May through October and a dry season the rest of the year (Fig. 2; Hastenrath 1967; Portig 1976). During the rainy season, the passage of transient weather disturbances across Central America and adjacent waters accounts for most of the synoptic timescale precipitation variability. These disturbance include meridional displacements of the intertropical convergence zone (ITCZ), hurricanes, tropical storms and depressions, and easterly waves. Caribbean easterly waves are the most frequent synoptic-scale weather disturbances that modulate rainfall over Central America. According to National Hurricane Center statistics, about 60 tropical

waves per year reach the eastern part of Central America (Frank 1976; Avila and Pasch 1992; Pasch et al. 1998). They are especially frequent during August and September, when the instability processes that produce these waves are most intense. These waves may induce meridional displacements and evolution of the ITCZ over the far eastern Pacific. In this region the ITCZ is a wide region composed of cloud clusters that undulate and, depending on ambient conditions, break into tropical disturbances or tropical cyclones (Nieto Ferreira and Schubert 1997). Portions of these systems can affect Central American rainfall.

The effect of hurricanes and tropical depressions on Central American rainfall has been documented for particular events (Fernández and Barrantes 1996; Fernández and Vega 1996; Hellin et al. 1999; Bell et al. 1999). Heavy rains combined with mountainous terrain, common in Central America, produce floods and landslides, often with major loss of life. The recent and most important example of this was Hurricane Mitch during 1998 (Hellin et al. 1999; Bell et al. 1999), where most of Central America was seriously affected by floods and landslides instigated by heavy rainfall. Fernández and

*Corresponding author address:* Michael W. Douglas, National Severe Storms Laboratory, 1313 Halley Circle, Norman, OK 73069.
E-mail: Michael.Douglas@noaa.gov

(a)



MONTHLY RAINFALL IN TENTHS OF PERCENT OF THE ANNUAL TOTAL IN THE PACIFIC REGION OF CENTRAL AMERICA



FIG. 2. Monthly mean rainfall histogram in tenths of percentage of the annual total for the Pacific region of Central America. Values from Portig (1976).
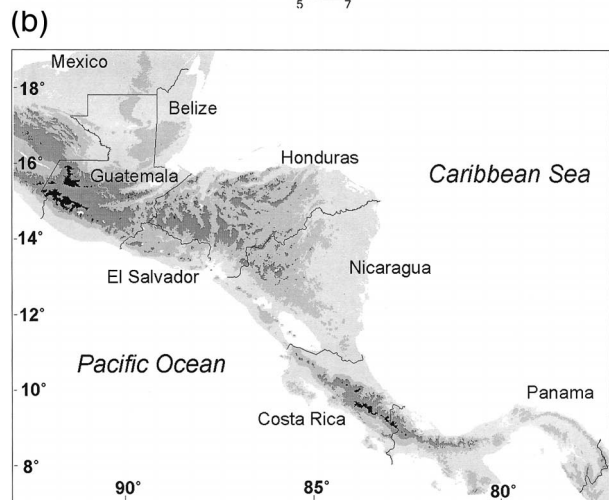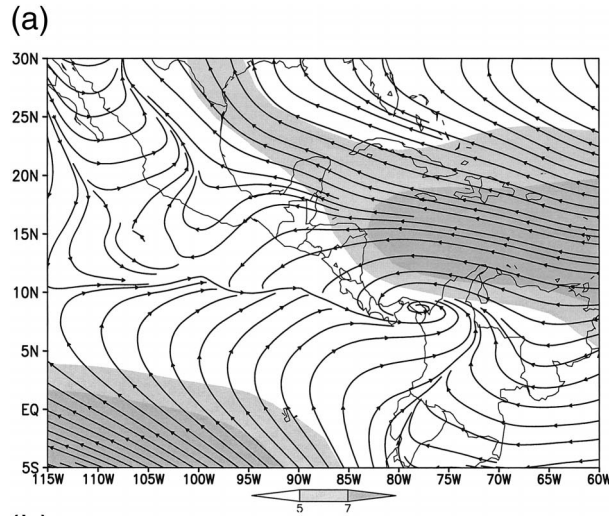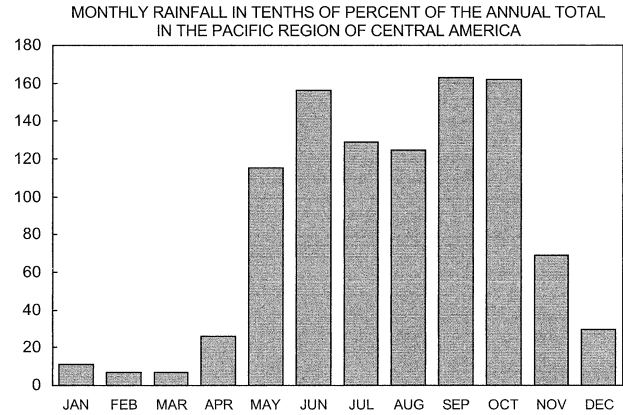
(b)



FIG. 1. (a) Long-term mean streamlines and isotachs at 925 hPa from the NCEP reanalysis data for May–Oct (rainy season). Light shading is area with wind speed greater than 5 m s$^{-1}$, dark shading is greater than 7 m s$^{-1}$. (b) Major elevation zones of Central America. Light shading is for areas above 500 m, intermediate shading is for above 1000 m, and dark shading is for above 2000-m elevation.

exceed 100 mm day$^{-1}$ at stations on the Pacific side of Central America (Fernández and Vega 1996).

A term commonly used in Central America to refer to persistent overcast or rainy weather conditions that may last from several days to more than a week is the *temporal*. This phenomenon occurs mainly during the months of June, September, and October (Hastenrath 1985) and has devastating effects on the Pacific side of Central America as it produces rainfall amounts similar to those of hurricanes. Temporales became the focus of investigations during the late 1950s (Portig 1958) and more actively in the 1960s (Lessmann 1964; Pallmann and Murino 1967; Pallmann 1968a,b). Lessmann (1964) pointed out that almost all temporales originated from the eastern Pacific ITCZ and mentioned that some were induced by hurricanes that move over the western Caribbean or pass over the Central American isthmus. Using surface data and satellite imagery from the *Nimbus*
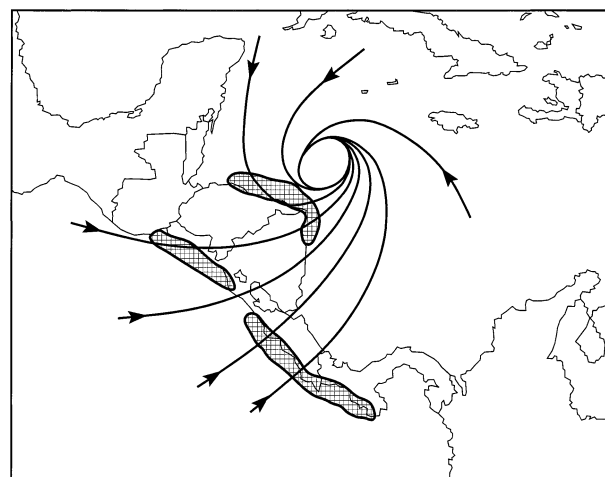
Barrantes (1996) divided the rainfall over Central America associated with tropical cyclones into "direct" and "indirect" effect. The direct effect, produced by the passage of the eyewall and spiral bands, is responsible for an enormous amount of rainfall on the windward side of mountain ranges. The indirect effect, resulting from the interaction of the large-scale circulation of the cyclone with the lee side of the mountains of Central America, can also produce large amounts of rain. Figure 3 shows a schematic of the two effects. Tropical cyclones that have the greatest effect on Central America are those with tracks over the southern part of the Caribbean Sea. They usually make landfall as far south as Central Nicaragua [~12°N; Aberson (1998)]. Tropical storms rarely pass over southern Central America but the indirect effects may produce large amounts of rain over the region. Rainfall in these circumstances may



FIG. 3. Schematic of the streamlines of a tropical cyclone over the Caribbean Sea and its "direct" and "indirect" effects on Central America. Hatched areas represent the regions of heavy rainfall produced by these effects.

*II* satellite, Pallmann and Murino (1967) and Pallmann (1968a,b) produced a synoptic and dynamic model to explain cloud formations associated with temporales. More recently, Fernández and Barrantes (1996) and Galo et al. (1996) used the conventional radiosonde network to document synoptic aspects associated with the temporales that occurred during May 1983 and October 1985, respectively. These later studies showed the importance of the southwesterly flow from the eastern Pacific as the main supplier of moisture for these rain systems. These later studies have also tended to minimize the temporal as a distinct category of synoptic system, as many temporales are apparently associated with the indirect effect of a tropical storm over the western Caribbean Sea.

Descriptions of seasonal-scale aspects of Central American rainfall in terms of satellite-derived data have been given by Arkin and Meisner (1987) and Garreaud and Wallace (1997). The former study emphasized the annual cycle of cold cloudiness over the Americas at a relatively coarse resolution (2.5° lat–long) while the latter study used imagery interpolated to 55-km spatial resolution to describe the mean and diurnal variation of rainy season cloudiness over the tropical Americas. Garreaud and Wallace's study emphasized the strong diurnal cycle over both the landmass of Central America and over the adjacent oceanic areas. These patterns of cloudiness appeared to be strongly influenced by the details of the topography and the geometry of the coastlines, suggesting that land–sea and mountain–valley breezes were very important for explaining the detailed distribution of cloudiness. Also, as both of these studies averaged cloudiness data over periods of months, it was not possible to investigate synoptic or intraseasonal variations in cloudiness.

Previous studies of Central American rainfall variability have generally lacked a sufficiently dense network of atmospheric soundings to define the characteristics and evolution of the circulations associated with these events. While some upper-air observations are made routinely around the Caribbean Sea and over Central America, aerological data are not routinely available over the eastern Pacific. Furthermore, the current model-based analyses that are used by researchers for climate studies lack upper-air in situ observations in the region that might help assess the accuracy of the analyses to represent the conditions associated with these rainfall variations. With the hope of partially alleviating this deficiency an economical upper-air sounding network, called the Pan American Climate-Sounding Network (PACS-SONET; Douglas and Fernandez 1997), was established during the rainy season of 1997. The network consisted of 12 pilot balloon stations (used to obtain wind profiles) and one radiosonde station (with wind, temperature, and humidity data) deployed from southern Mexico to northern Peru (Fig. 4). While the observations were intended for a variety of climate-related stud-
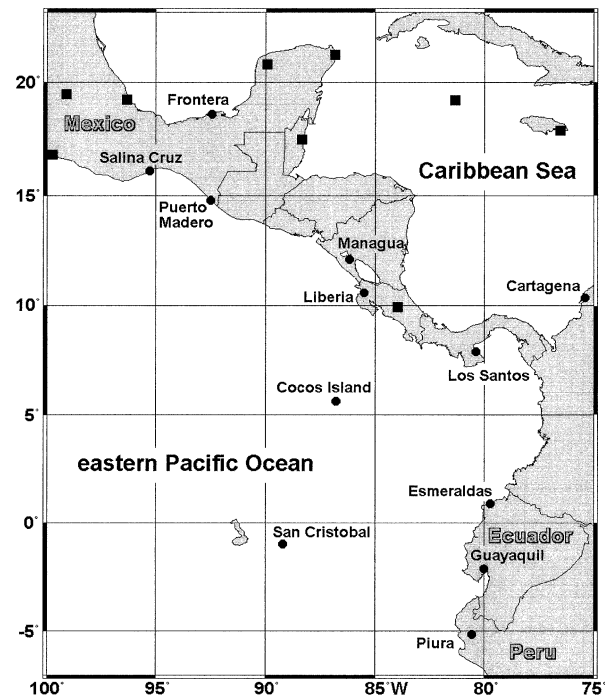


FIG. 4. The PACS-SONET sounding network during the summer season of 1997. Black dots show the location of the PACS-SONET pilot balloon observations. Black squares show the locations of radiosonde stations from the conventional network.

ies the data can also be used to study the wind field structure of synoptic-scale disturbances.

The present study is a multifaceted approach involving the blending of surface rainfall observations, upper-air wind measurements, and outgoing longwave radiation (OLR) from National Oceanic and Administration (NOAA) polar-orbiting satellites (Gruber and Winston 1978; Gruber and Krueger 1984; Liebmann and Smith 1996) to describe typical conditions associated with wet and dry spells over Central America. Both wind and OLR analyses are based on a compositing technique, which involves first the selection of meteorological events with similar characteristics and then obtaining averaged characteristic of these events. This procedure can improve the "signal to noise ratio" that is a well-known deficiency of individual case studies where the observations are not spatially dense or temporally frequent. Compositing also tends to identify the aspects of a phenomena that are common to most events, and diminishes characteristics that might be restricted to particular events. This investigation focuses on wet and dry spells that occurred over the Pacific side of Central America during the rainy seasons (May–October) of 1990–94 and 1997. Upper-air observations from the enhanced network during the rainy season of 1997 permit more detailed examination of the wind field associated with wet and dry spells than previously possible. OLR data, together with rainfall data from Central America, were also used to determine characteristics of the wet

and dry spells. Finally, National Centers of Environmental Prediction–National Center of Atmospheric Research (NCEP–NCAR)-hereafter referred to as NCEP) reanalysis data (Kalnay et al. 1996) were used for comparison with the observations made during 1997 to determine whether these latter, widely used data also depict the differences between wet and dry spells. The analyses using data from the enhanced network serve as an independent source for comparison with the NCEP reanalysis data, since the PACS-SONET observations were not available for ingestion into the NCEP data assimilation system. The NCEP reanalysis data were also used to evaluate whether the characteristics of wet and dry spells during the rainy season of 1997 are representative of other years.

The specific objectives of this study can be summarized as an attempt to determine 1) the large-scale wind field associated with wet and dry spells using data from the 1997 enhanced upper-air network (conventional radiosondes and special PACS-SONET), 2) whether the NCEP reanalyses capture the same atmospheric characteristics as those observed by the enhanced observing network, and 3) the spatial extent and vertical structure of wet and dry spells by means of composites of reanalysis data and OLR fields. The paper is organized as follows: section 2 describes the data and methodology, section 3 discusses the temporal distribution of the wet and dry spells, and section 4 discusses the wind field composite of wet and dry spells using the 1997 enhanced upper-air network and compares this composite with another using the NCEP reanalysis data. Section 5 uses the NCEP reanalysis and OLR data to examine the spatial extent and general characteristics of the wet and dry spells of 1997 and 1990–94, and section 6 summarizes the results.

## 2. Data and methodology

### a. Overall procedure

This study is based on two distinct sources of information: six rainy seasons (1990–94, 1997) of observed daily rainfall obtained from the national meteorological services in Nicaragua, Costa Rica, and Panama, and one rainy season (1997) of upper-air wind data obtained from the PACS-SONET field experiment. These datasets are complemented with radiosonde data from stations throughout the region, daily averaged values of wind and specific humidity from the NCEP reanalysis data, and daily averaged OLR. The study emphasizes the wind field at 925, 850, 700, and 500 hPa. Surface and 1000-hPa wind data were not used in this study because, except over ocean regions, topographic effects over Central America make near-surface wind observations generally unrepresentative and very difficult to use in synoptic analysis.

Wet and dry spells were identified from the time series of rainfall data reported at a large number of rain gauge stations. Wet days were defined as the days in the time series that had 75% or more stations reporting rain; dry days were those days with 35% or less stations reporting rain. The thresholds (75% and 35%) were chosen so that the number of samples was large enough to make a reliable composite but not so large to prevent identifying differences between wet and dry spells. When the length of a wet spell lasted more than a day, the first day that equaled or passed above the 75th percentile was considered the first day in the wet spell. Likewise the first day in a dry spell was the one which first equaled or passed below the 35th percentile. These definitions of "wetness" or "dryness" minimize the sensitivity to isolated heavy rainfall events. The *wettest* day was considered the day, within the wet spell, when the largest number of stations reported rainfall. Similarly the *driest* day was that which had the smallest percentage of stations reporting rainfall. As it will be seen in section 3, the time interval between two successive wettest or driest days is at least 3 days but often is 5 days or more.

Once the dates of the wettest and the driest days were identified a compositing analysis was performed using the wind field at different pressure levels from both the enhanced sounding network and the reanalysis. A compositing analysis was also performed using specific humidity from the reanalysis and OLR field. Data availability restricted this study to consider only observed wind field composites for the season of 1997.

Average values of the aerological data, consisting of conventional radiosonde plus special pilot balloon observations (Fig. 4), during wet and dry spells, were plotted and subjectively analyzed. The wind field differences between wet and dry spells, at different pressure levels, were also calculated for each station and analyzed to better distinguish the circulation patterns associated with wet and dry spells. These analyses were contrasted with their counterpart analyses using the NCEP reanalysis data that have been produced for research into climate variability. In addition to these horizontal analyses, vertical profiles of the horizontal wind were prepared for key stations to show the strength and depth of critical tropospheric mass fluxes associated with wet and dry spells.

### b. Rainfall data

Ground-based rainfall observations were used to identify the temporal and spatial distributions of wet and dry spells. This allows for a selection of wet and dry spells independent of assumptions such as the cloud-top temperature or type and size distribution of the cloud droplets that are used to estimate rainfall from satellite or radar remote sensors. However there are usually a number of problems that have to be considered when using this approach. The rain gauge network has an uneven distribution; that is, there is no information over the ocean, and the land stations are often located close to populated areas, rather than being uniformly dis-

TABLE 1. Number of rain gauge stations used in this study in Nicaragua, Costa Rica, and Panama for the rainy seasons of 1990–94 and 1997.

| Year | Nicaragua | Costa Rica | Panama | Total |
|------|-----------|------------|--------|-------|
| 1990 | 9 | 35 | 19 | 63 |
| 1991 | 53 | 35 | 15–17 | 104 |
| 1992 | 86 | 35 | 18 | 139 |
| 1993 | 100 | 35 | 16–17 | 151 |
| 1994 | 107 | 35 | 15–16 | 157 |
| 1997 | 16 | 18 | 15 | 49 |

tributed. Rain gauge observations, because of local effects, often are not representative of large regions. Thus, a calculation of areal mean rainfall may not be reliable. Finally, the convective nature of the rainfall over the Tropics makes it difficult to sample adequately rain-producing disturbances. Fortunately, the above-mentioned problems have not seriously affected this study since the main use of the rainfall data has been to determine when rainfall was present or absent at the stations.

Daily rainfall data were obtained from four Central American institutions; the Instituto Nicaraguense de Estudios Territoriales (INETER) in Nicaragua, the Instituto Meteorólogico Nacional (IMN) in Costa Rica, the Instituto de Recursos Hidráulicos y Electrificación (IRHE), and the Panama Canal Commission in Panama. The number of raingauge stations from each country that were used in this study is shown in Table 1. The numbers in this table do not represent all of the data gathered, but only the data that were in a digital, or at least organized, format. All stations located on the Pacific side of Central America were selected. While the topography (Fig. 1b) allowed for easy distinction of the Pacific and Caribbean sides of Central America in Costa Rica, Panama, and in northern Nicaragua, the flat terrain in southern Nicaragua made it necessary to define a threshold longitude, which was chosen as 85°W. Figure 5 shows the locations in the rain gauge station network for 1997. The distribution of stations for the five rainy seasons, 1990–94, was the same in Costa Rica and nearly the same in Panama; however, it varied from year to year in Nicaragua. Despite this variation in reporting, all stations were taken into account because the primary interest was to know whether or not rainfall was observed. Since the rainfall data came from different sources, it was first organized into a standard format. The dataset was then arranged to show the number of stations that reported rainfall for each of the days in the database. A time series of the percentage of stations reporting rainfall was then prepared for each of the 6 yr. The time series start on 1 May and continue through 31 October (185 days total). Since the number of stations in the database during 1990–94 was variable (e.g., during 1993, Nicaragua had 100 stations while Panama had only 17), the percentage for each country was first calculated; from these values the average percentage of
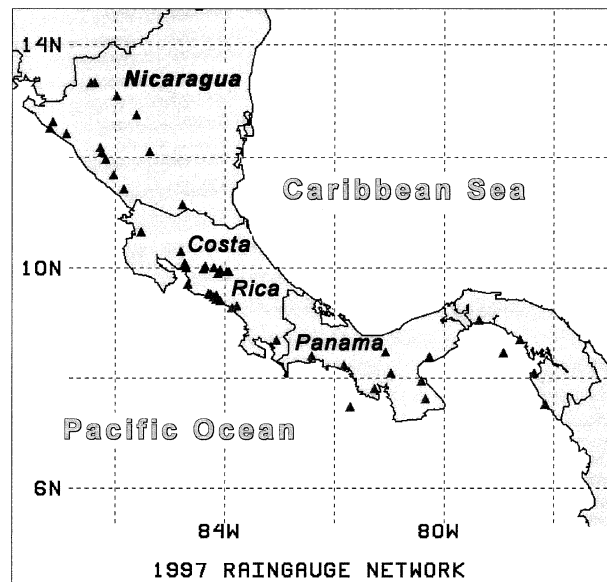


FIG. 5. Location of the rain gauge stations for the rainy season of 1997.

the three countries was then calculated. For the year 1997 the number of stations in each country was similar; therefore, the previous procedure was not necessary.

### c. Upper-air wind data

As discussed in the introduction, this study was, in part, made possible by the implementation of an enhanced upper-air network over Central America and the eastern tropical Pacific that operated during the Central American rainy season (May–October) of 1997. Pilot balloon observations were made at 13 stations from southern Mexico to northern Peru. Two of these stations were located on islands in the eastern Pacific: Cocos Island, Costa Rica, and San Cristobal (Galapagos Islands), Ecuador. Pilot balloon observations were made instead of radiosonde observations at nearly all sites not only because of the limited budget available for the observing program, but because pilot balloon observations require relatively little training, and the equipment (optical theodolites obtained on loan from the National Weather Service) is robust, requires no electricity, and is easily transportable (Douglas 1991). Also, small balloons can be used, so that no special inflation shelters were needed and gas transportation problems were minimized.

The pilot balloon observations during 1997 were made twice daily, early in the morning (~1200 UTC) and later in the afternoon (~0000 UTC), when the assumed constant ascent rate of the balloons (estimated previously from double theodolite tests) is less affected by turbulence induced by heating of the surface. The elevation and azimuth angles obtained by tracking the balloon (every 30 s in the first 8 min and every 1 min

afterward) with the meteorological theodolite were recorded by hand and sent to centers in each country where the data were processed. Using an interactive computer program the angles were displayed and corrected for obvious errors. The wind was then calculated by assuming that the balloon ascent rate was constant. After this, the wind data were sent via the Internet to the National Severe Storms Laboratory (NSSL), where it was posted on a Website (http://www.nssl.noaa.gov/projects/pacs) for access by the scientific community. Wind data from this network were obtained with relatively high vertical resolution (every ~200 m) in the lower troposphere. The main limitations of this type of measurement are the lack of moisture information and the requirement of fair weather at the time of observation (the observers have to visually track the balloon). Surprisingly, the negative impact of cloudiness at many sites was less than might be expected at tropical locations. This was because the hours of observation, early morning and late afternoon, generally are times of minimum boundary layer convection (and cumulus formation), which is usually strong during the midday.

Upper-air data from the routine World Weather Watch (WWW) radiosonde network was obtained from the National Oceanic and Atmospheric Administration's (NOAA) Forecast Systems Laboratory via their Web site (http://www.fsl.noaa.gov). Unfortunately, most stations in the Caribbean Sea region and in Central America lost wind information after 30 September 1997, owing to the shutdown of the Omega Navigation system. The higher spatial resolution of the enhanced network prior to this date provides a unique opportunity to study the large- and regional-scale structure of atmospheric circulations associated with rainfall variability over Central America.

Composites were produced of the upper-air circulation associated with the 13 driest days and 18 wettest days identified during the rainy season of 1997. To do this, the PACS-SONET pilot balloon observations were merged with the conventional radiosonde network data. Since the wind data from pilot balloon observations are given as a function of height instead of pressure, climatological values of the height of the pressure levels were used to convert these values to pressure levels. Also, to slightly smooth the pilot balloon wind data the average of a layer (with thickness of almost 10% of the height value, rather than a single observation) was matched with the closest mandatory pressure level. Pilot balloon morning observations (regularly made after sunrise, from 1200 to 1400 UTC) and late afternoons (from 2330 to 0030 UTC) were blended with corresponding 1200 and 0000 UTC radiosonde data, respectively. Wind field analyses for both the wettest and the driest days were obtained for the standard levels at 850, 700, and 500 hPa. To show more clearly the difference between wet and dry spells, analyses of the difference between wet and dry wind fields were also made. Analyses above 500 hPa are not discussed here because the number of

pilot balloon observations was often below five at a number of stations, making the composites less reliable. In addition to horizontal analyses of the wind field, mean profiles of the wind for particular stations were plotted for the wet and dry spells as well as the daily sequence around the wettest and driest days.

### d. NCEP reanalysis and OLR data

The NCEP reanalysis uses a frozen state-of-the-art global data assimilation system and more data than is available for the operational analysis (see Kalnay et al. 1996). The main source of the upper-air data used for the reanalysis is the rawindsonde data composed of Global Telecommunications System (GTS) transmitted data and that obtained from national archives. Satellite cloud drift winds complement the upper-air wind field data in the reanalysis. The NCEP reanalysis data is used in this study for two principal objectives, the first is to compare the reanalyzed wind fields with wind analyses generated from the enhanced sounding network data discussed in the previous subsection. The second main objective of using reanalysis data is to use the analyzed and derived fields, together with OLR data, to provide a more comprehensive picture of the wet and dry spells, particularly for the rainy seasons of 1990–94. OLR anomalies have been used in many studies (e.g., Xie and Arkin 1998) as a proxy for rainfall at low latitudes where precipitation is primarily from deep cumulonimbus convection.

Daily averaged NCEP reanalysis and OLR data were obtained from the Climate Diagnostics Center (CDC) Web site (http://www.cdc.noaa.gov). All of the quantities are available on a 2.5° latitude by 2.5° longitude grid spacing. Composites of the wind field, moisture, horizontal moisture flux, and moisture convergence field for wet, dry, and wet minus dry spells were made for the mandatory levels at 500 hPa and below. OLR was similarly composited with respect to the dry and wet spells, and difference fields were generated.

### 3. Temporal distribution of wet and dry spells

A time series plot of the percentage of stations reporting rainfall for the rainy season (May–October) of 1997 is shown in Fig. 6. The time series seems to delineate two modes of variation, one with a timescale of 1–2 months and another, of higher frequency, with a timescale of slightly less than a week. Comparison of the 1997 rainfall data with time series from the years 1990–94 (not shown) shows similarities, despite interannual variation in the number of wet and dry spells (see Table 2). Common characteristics include (i) wet spells usually occur after the second week of May, decrease in number during July and increase again reaching a maximum number during September, and (ii) dry spells occur during the first 3 months of the rainy season with the highest frequency during late May and July.
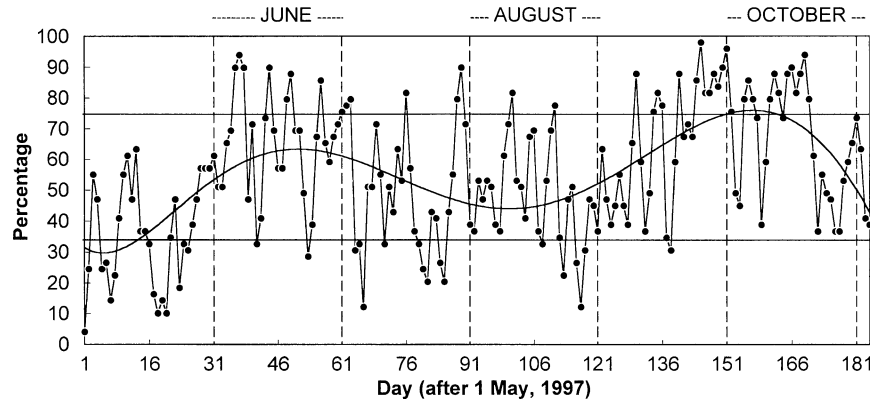
Fig. 6. Percentage of stations reporting rainfall over the Pacific region of Central America for the rainy season of 1997. Solid line represents a 6° polynomial fit to the data to suggest seasonal trend and intraseasonal variation.

The increase in the percentage of stations reporting rainfall during May coincides with the northward migration of the ITCZ over the eastern Pacific to near 8°N.

The large number of wet spells during September and October may be associated with either the more frequent passage of easterly waves across the region (e.g., Avila and Pasch 1992, 1995) or to periods of tropical cyclogenesis over the eastern Pacific. Except for 1993, September had the maximum number of cyclone events in the years considered in this study (Rappaport and Mayfield 1992; Lawrence and Rappaport 1994; Avila and Mayfield 1995; Pasch and Mayfield 1996). Also, the high frequency of wet spells in the months August–October may be associated with higher overall SSTs in the region and an ITCZ closer to Central America (Sadler et al. 1987). Dry spells occurred often during July and August, and are indications of the midsummer drought phenomenon (Magaña et al. 1999).

Although wet spells were defined in terms of the percentage of stations reporting rainfall, rather than the amount of rain observed in the database, wet spells may account for a large percentage of the monthly rainfall during the rainiest months of the year. Table 3 shows the daily rainfall for each of the months considered in this study and the daily rainfall averaged over the wet periods. It is clear that during wet spells the rainfall can be more than twice as high as that observed for an average day.

## 4. Analysis of the wind field during 1997

### a. Wind field composites of wet and dry spells

As discussed in section 2a the wettest and driest days identified in the wet season of 1997 were chosen to produce upper-air wind field analyses. The same dates were used to make wind field composites using the NCEP reanalysis data. To highlight the differences between the wet and the dry days in the wind field we show only the analyses of wet minus dry wind fields. The departure of a dry or wet day from the mean determined as the average of wet and dry day conditions would then be half the values shown.

In order to show the differences between analyses based on the upper-air observations and the NCEP reanalyses, both sets of analyses are described together rather than separately. The comparison of the NCEP reanalyses with analyses based on direct sounding information (including the PACS-SONET data) was an important object of the sounding program, especially over the normally data-void eastern Pacific. It was not obvious that the NCEP reanalyses would provide realistic depictions of the wind field over the far eastern Pacific.

### 1) 850-HPA ANALYSIS

The 850-hPa level (very similar to the 925-hPa level; not shown) is the level of greatest confidence, as the

TABLE 2. Number of wet/dry spells identified in the time series of the percentage of stations reporting rainfall for the rainy seasons of 1990–94 and 1997. The last column shows the total number of wet/dry spells for the given rainy season, and the row at the bottom shows the total number of wet/dry spells per month.

| Year | May | Jun | Jul | Aug | Sep | Oct | Total per year |
|---|---|---|---|---|---|---|---|
| 1990 | 2/5 | 0/3 | 0/5 | 2/0 | 3/0 | 4/1 | 11/14 |
| 1991 | 2/3 | 2/1 | 1/4 | 2/4 | 2/2 | 0/1 | 9/15 |
| 1992 | 0/6 | 1/2 | 2/2 | 0/2 | 2/0 | 1/2 | 6/14 |
| 1993 | 2/1 | 4/3 | 2/3 | 5/2 | 4/0 | 2/1 | 19/10 |
| 1994 | 0/2 | 1/2 | 0/1 | 3/0 | 2/0 | 4/1 | 10/6 |
| 1997 | 0/4 | 4/1 | 3/4 | 2/3 | 5/1 | 4/0 | 18/13 |
| Total per month | 6/21 | 12/12 | 8/19 | 14/11 | 18/3 | 15/6 | 73/72 |

largest number of pilot balloon observations are present at this level. The wet minus dry analysis (Fig. 7a) indicates that during wet spells there is both stronger cross-equatorial flow and anomalous westerly winds across Central America and much of the Caribbean Sea. The opposite anomalous wind flow is suggested for dry spells. A region of cyclonic streamline curvature is evident offshore western Mexico. Many of the main differences between wet and dry spell composites such as the cross-equatorial flow and the Caribbean trade winds are also depicted by the reanalysis data (Fig. 8a). Although at this level the agreement between the wind field from the sounding network and the reanalysis is better than at other levels over the eastern Pacific there are still differences. For example, the reanalysis shows a weaker southerly wind component near the equator than that suggested by the soundings.

### 2) 700-HPA ANALYSIS

The dominant aspect of the wet minus dry wind field at 700 hPa (Fig. 7b) is the southerly winds over the eastern Pacific that become westerly as they pass over Central America. As at 850 hPa, the westerly wind anomaly observed over Central America extends eastward, as far as the eastern Caribbean Sea, indicating that wet and dry spells are associated with large-scale variations in the trade wind flow. The westerly wind anomaly over Central America and the Caribbean Sea is also well represented by the NCEP reanalysis (Fig. 8b). Over the eastern Pacific, however, the NCEP reanalysis data do not indicate the significant southerly wind component that is shown by the observations at San Cristobal and Cocos Island (section 4b).

### 3) 500-HPA ANALYSES

The difference between wet and dry composite wind fields at 500 hPa (Fig. 7c) shows a large cyclonic circulation anomaly, with its center just northeast of Honduras. Associated with this circulation anomaly is anomalous northwesterly flow over Central America. An east–west axis of cyclonic shear is observed from western Mexico to the eastern Caribbean Sea. Confluence of the anomaly streamlines over the Panama–Colombia border is also evident. The NCEP reanalysis–based difference analysis (Fig. 8c) shows reasonably good agreement with the observed differences. The cyclonic circulation over the western Caribbean and the cyclonic shear flow over the eastern Caribbean are in particular quite similar to those features in Fig. 7c. The center of the circulation over the Caribbean, however, is located more to the north in the reanalysis composite than the observations indicate. In the eastern Pacific, south of Baja California, the reanalysis data show a cyclonic circulation anomaly—something that is weakly suggested from the sounding data. Over the eastern Pacific the reanalysis composite displays a strong westerly

anomaly that extends far to the west and south, while the observation-based wind anomaly at San Cristobal (Fig. 7c) suggests a northwest anomaly.

### b. Eastern Pacific cross-equatorial flow

An important feature associated with the enhancement of convective activity over the Tropics, especially near-equatorial regions, is the airflow across the equator (Ramage 1971). In the western Pacific and Indian Ocean, the cross-equatorial flow is associated with the seasonal rainfall over Indonesia, southern China, India, and eastern Africa. In the western Pacific, enhanced cross-equatorial flow is often associated with the genesis of typhoons (Wang and Leftwich 1984). In the eastern Pacific the low-level cross-equatorial flow is an almost permanent feature. Near the equator the cross-equatorial flow has a typical depth of 1 km (Hastenrath 1985) and monthly mean surface wind speeds below 6 m s$^{-1}$ (Sadler et al. 1987) during the Central American rainy season. Pallmann (1968a,b) attempted to relate cross-equatorial flow in the eastern Pacific with the development of temporales over Central America, and persistent heavy rainfall over the Pacific side of Central America was thought to be the product of polar surges from the Southern Hemisphere. Lack of observations over the region prevented evaluating Pallmann's hypothesis.

From the analysis of the wind field difference (wet minus dry) at 850 and 700 hPa (Figs. 7a,b, respectively), it is apparent that the cross-equatorial flow is a key feature that distinguishes wet spells from dry spells. Vertical profiles of the meridional wind during wet and dry days at three near-equatorial PACS-SONET pilot balloon sites (Fig. 9) better display the vertical structure of the meridional flow. During wet spells the depth of the low-level cross-equatorial flow over San Cristobal and Esmeraldas is about 2 and 1.2 km, respectively; this is more than 400 m deeper than during dry spells. The strength of the meridional flow at these two stations is, throughout much of the boundary layer, about 2–3 m s$^{-1}$ larger during wet spells than during dry spells. Another layer of southerly cross-equatorial flow is found over San Cristobal between 1.8 and 3 km ASL. Such a layer does not appear 1 day before nor 1 day after the wettest day; however, 9 out of the 10 observations for this layer on the wettest day showed this second increase in the southerly flow at San Cristobal. Consistent with the stronger and deeper cross-equatorial flow near the equator during wet spells is the stronger and deeper southerly flow observed over Cocos Island. During dry spells weak northerly flow is observed in the lowest 3 km at this island. A 3-day sequence of the meridional wind profiles for both wet and dry spells at San Cristobal (Fig. 10) shows that the strength and depth of the low-level cross-equatorial flow are similar in the days before and after the wettest and driest days. Thus, fluctuations in the meridional wind component at San Cristobal associated with wet and dry spells have timescales longer

(a)



wet-dry streamlines
850 hPa

• ddd ff

ddd is direction in degrees
ff is speed in knots (1 kt ~.5m/s)

(b)



wet-dry streamlines
700 hPa

• ddd ff

ddd is direction in degrees
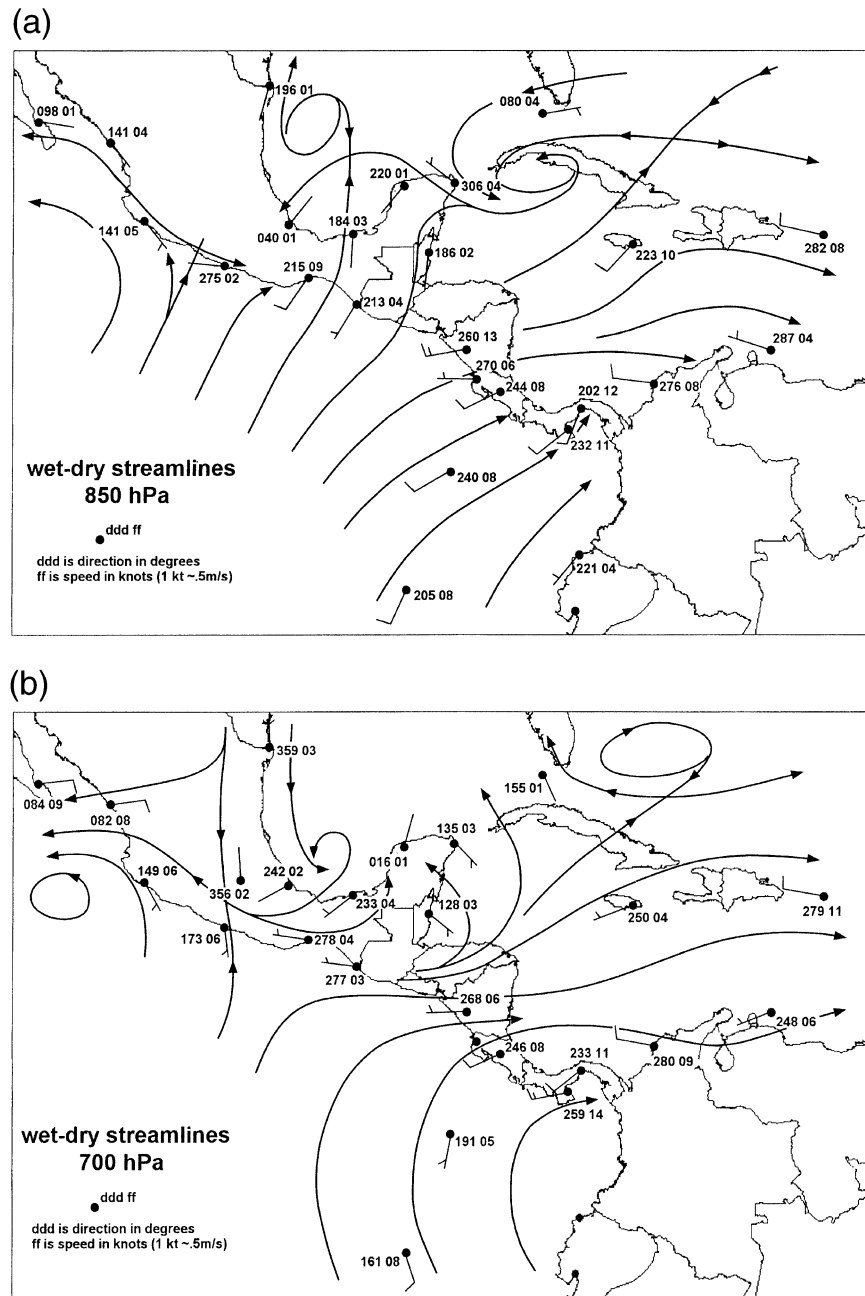ff is speed in knots (1 kt ~.5m/s)

FIG. 7. Wind field difference composite of 18 wet and 13 dry spells during the rainy season (May–Oct) of 1997 using the enhanced sounding network data. Direction in degrees, speed in kt (2 kt ~ 1 m s$^{-1}$): (a) 850, (b) 700, and (c) 500 hPa.

than a day. Figure 10 also indicates that the strongest cross-equatorial flow occurs 1 day before the wettest day and that the weakest flow occurs 1 day before the driest day. A plot of the mean meridional flow in the surface to 1 km ASL layer at San Cristobal relative to the wettest and driest days (Fig. 11) supports the previous assertion. It also suggests an approximately 1-week periodicity in the intensity of the cross-equatorial flow over San Cristobal, if the second day after the driest

day is merged with the second day before the wettest day, as shown in Fig. 11.

A comparison between the pilot balloon observations of the wind at San Cristobal (0.9°S, 89.6°W) and the reanalysis wind profile at the closest grid point (0°, 90°W) (Fig. 12a) shows that the main features of the low-level southerly flow during wet and dry spells are captured in the reanalysis data. As in the observed data, stronger and deeper southerly flow is evident during wet

(c)
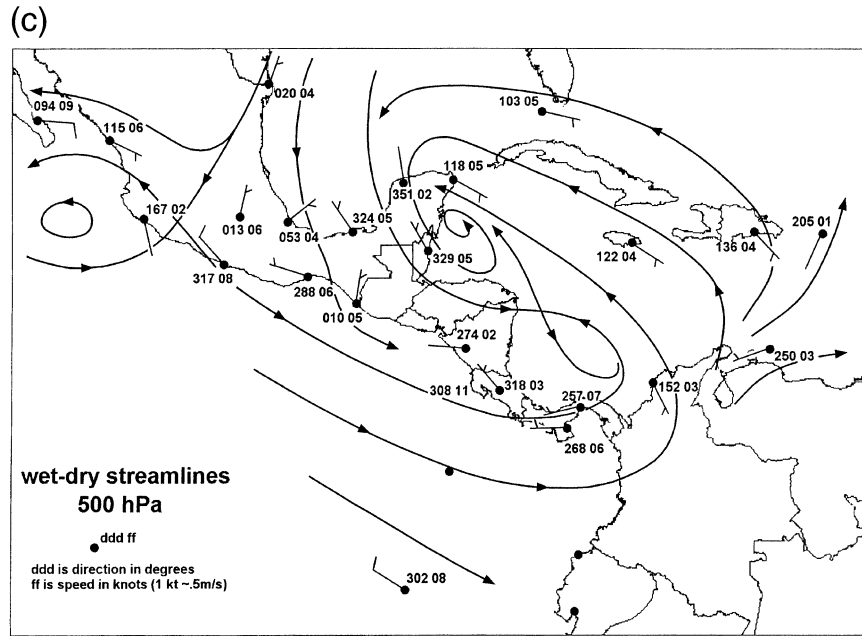


FIG. 7. (*Continued*)

spells. The low vertical resolution of the available re-analysis data (compared with the observations) prevents the definition of the observed cross-equatorial flow maximum within the lowest-1-km layer. A large difference is found at about 3 km ASL (near 700 hPa) for the wet spell composite with much weaker than observed southerly flow in the reanalysis. We compared observations with the reanalysis in other pilot balloon stations and found that, in general, the reanalysis is consistent with the observations but discrepancies exist in the lowest 1 km.

### c. The easterly trade winds

Central America is embedded in easterly trade wind flow for most of the year. Thus, it might be expected that there should be a correspondence between changes in the rainfall regime and variations in the prevailing trade winds. The seasonal variations in the intensity of the trade winds are associated with the month to month

TABLE 3. Average daily percipitation (mm day$^{-1}$) per station for Aug, Sep, and October for each of the years considered. In brackets are the average daily percipitation per station during wet spells. Note that no wet spells were identified during Oct 1991 and Aug 1992.

| Year | Aug | | Sep | | Oct | |
|---|---|---|---|---|---|---|
| 1990 | 9.1 | (18.4) | 11.0 | (19.3) | 15.9 | (21.1) |
| 1991 | 5.7 | (19.5) | 7.7 | (15.4) | 6.8 | (0) |
| 1992 | 5.1 | (0) | 9.8 | (21.7) | 6.0 | (15.8) |
| 1993 | 10.1 | (15.6) | 12.7 | (17.8) | 6.5 | (9.4) |
| 1994 | 6.3 | (9.6) | 8.4 | (14.3) | 8.9 | (17.8) |
| 1997 | 4.0 | (8.2) | 8.6 | (12.5) | 8.1 | (14.1) |

rainfall variation on either side of the Central American mountains. Dry months on the Pacific slopes coincide with stronger low-level easterly flow, while weaker winds are associated with wetter months. From the analyses of the wind field difference between wet and dry spells at 850 and 700 hPa (Figs. 7a,b), the same correspondence is evident for shorter timescale fluctuations. Stronger trades coincide with dry spells and weak trades with wet spells.

The vertical profile of the zonal wind at Cocos Island, Managua, and Los Santos illustrates the trade wind variations associated with wet and dry spells (Fig. 13). Although the low-level westerly wind anomaly (in the wet minus dry composite) is consistently observed in both the conventional radiosonde and PACS-SONET observations, the pilot balloon stations were chosen because of their higher vertical resolution in the lower troposphere and because of their better geographical setting relative to Central America (only Panama City, Panama, was a regular low-altitude radiosonde station in Central America during the summer of 1997). The largest difference in the zonal flow between wet and dry spells is observed at Managua, but differences in the strength of the trade winds are evident at Los Santos and Cocos Island as well. In Fig. 12b the vertical profiles of the zonal wind composite over Managua (12.1°N, 86.2°W) and over the closest grid point (12.5°N, 85°W) in the reanalysis data show good agreement near the surface and at the 3-km level. However, the observed strong easterly flow in the 1–3-km layer during dry spells is not well captured by the reanalysis. The observed easterly flow in this layer might be accentuated by the regional topography (see Fig. 1b) that apparently channels the trade winds.
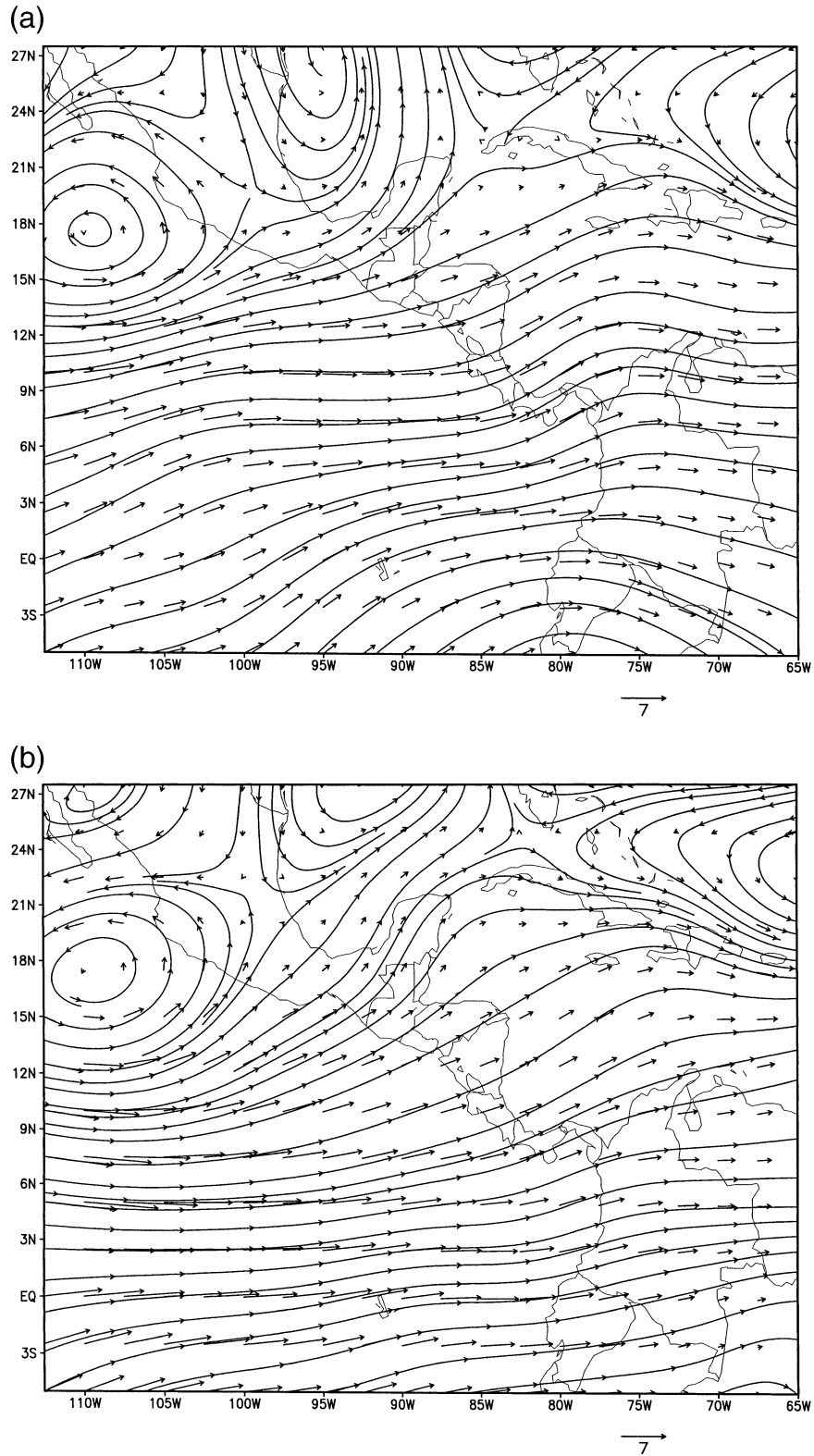
(a)

(b)

FIG. 8. Wind field difference composite of 18 wet and 13 dry spells during the rainy season (May–Oct) of 1997 using the NCEP reanalysis data. Vector at bottom in m s$^{-1}$: (a) 850, (b) 700, and (c) 500 hPa. Compare with Figs. 7a–c.
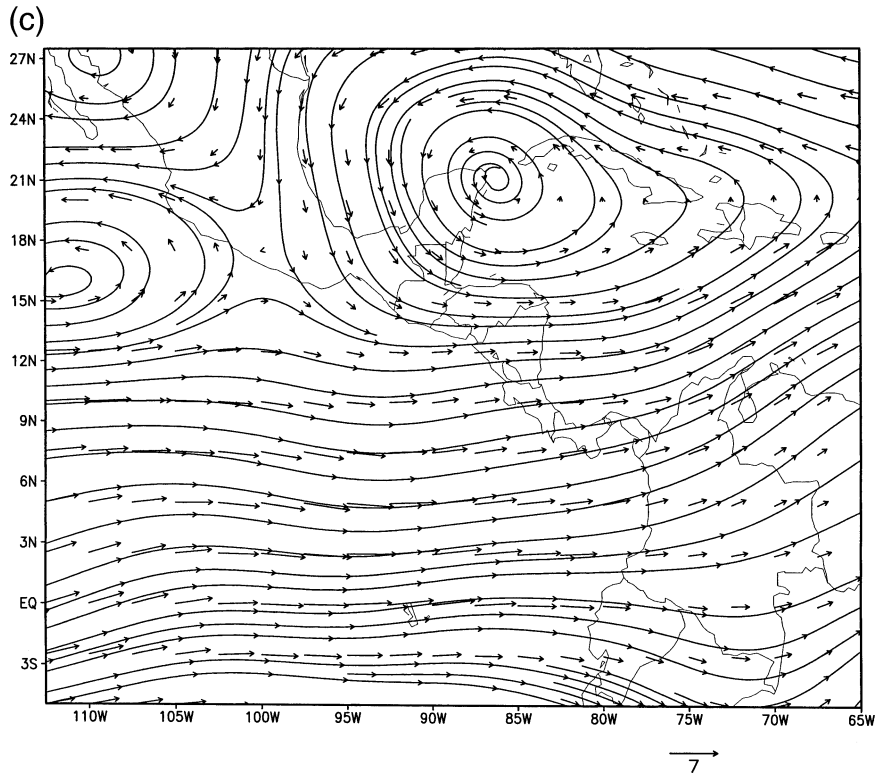
(c)



FIG. 8. (*Continued*)

A scatterplot of the easterly flow at 1512 m (~850 hPa) over Managua against the percentage of Central American stations reporting rainfall (Fig. 14) suggests an approximately linear relationship (with a correlation of 0.55) between the two quantities. In Fig. 14 it is clear that for extreme cases of westerly (instead of the usual ~7 m s$^{-1}$ easterly) flow over Managua wet spells are very likely to occur, and for stronger than normal easterly flow dry spells are very likely to happen. At least two mechanisms can be suggested that might explain this observation. One is that stronger northeasterly

winds over the Caribbean Sea and Central America are generally associated with stronger trade wind inversions and stronger subsidence on the synoptic scale (Riehl 1979), which tend to inhibit ascending motion and reduce convective activity. Another possible explanation is that stronger downslope motion associated with stron-
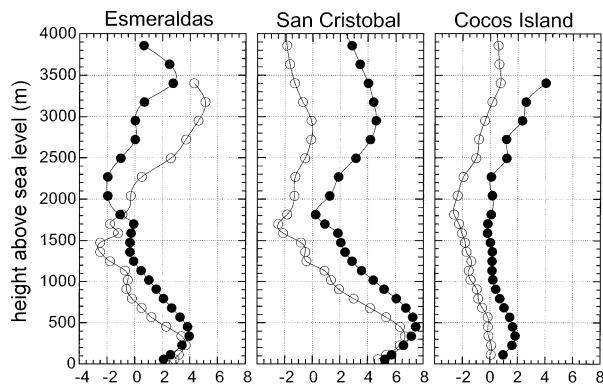


FIG. 9. Mean vertical profile of the meridional wind (in m s$^{-1}$) at Esmeraldas, San Cristobal, and Cocos Island during wet and dry spells. Solid dots are the wet spells; open circles are the dry spells. Means comprising less than five observations are not shown.
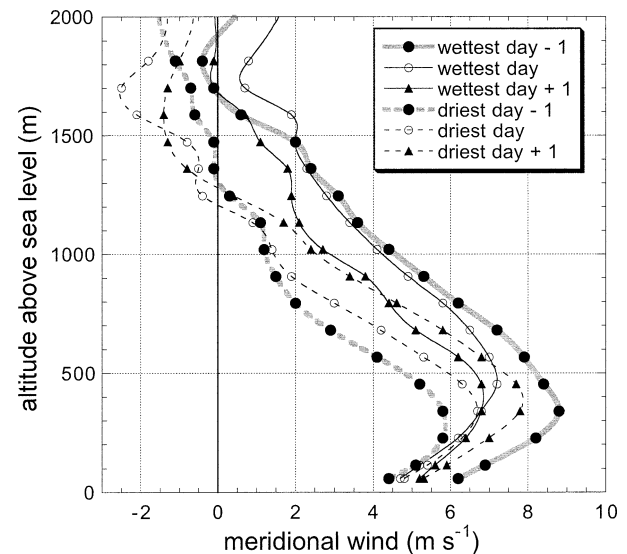


FIG. 10. Three-day sequence of the meridional wind at different heights over San Cristobal during (a) wet and (b) dry spells
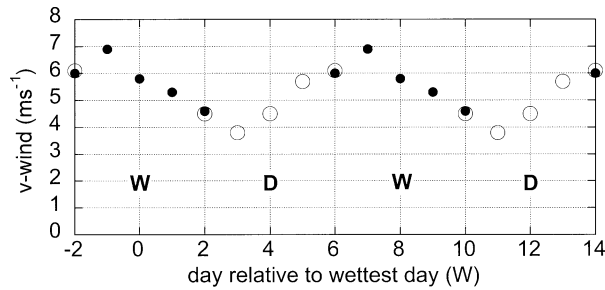
FIG. 11. Daily sequence (from two days prior to two days after the wettest or driest day) of the vertical profile of the meridional wind, integrated over the lowest 1 km, at San Cristobal. Solid dots are the days with respect to the wettest day (W), the open circles are the days with respect to the driest day (D). The values have been merged and overlapped to suggest periodicity, and two cycles are shown.

ger trade wind flow prevents the formation of clouds on the Pacific side of Central America. Quite possibly both processes occur together. A third possibility is that stronger trade wind flow weakens sea–land-breeze circulations that are due to daytime differential heating between land and ocean. The reduced ascent associated with these circulations would then produce less convective development, other factors being equal (Estoque 1962).

## 5. Wet and dry spells in the reanalysis and OLR fields

The previous section has shown that for the rainy season of 1997 the NCEP reanalysis captures the large-scale features of the wet and dry spells, which were defined by the fraction of stations reporting rainfall on any given day. In this section we use reanalysis and OLR data to test whether the wind field composites and the spatial extent of the OLR anomalies for the rainy season of 1997 are consistent with composites using a larger population of data, particularly the rainy seasons of 1990–94. In addition, aspects of the moisture field and moisture convergence from the NCEP reanalyses are presented with the object of understanding possible mechanisms that give rise to the observed rainfall variations.

### a. Wind field composites for 1990–94

The rainy season of 1997 was the focus of this investigation because the deployment of an enhanced sounding network provided enough observations to study the synoptic-scale variability of the wind field over Central America. However, the season presented very special conditions associated with the strong El Niño 1997–98 event. Thus, conclusions obtained from this period might not be true for other years. To estimate the representativeness of the 1997 data we used rainfall data for the rainy seasons of 1990–94 to identify, in the same way as in 1997, wet and dry spells and to generate
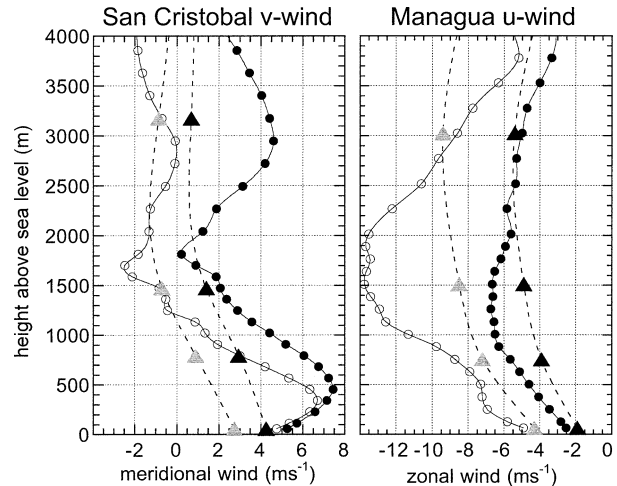


FIG. 12. Comparison of observed (dots) and NCEP reanalysis (triangles) mean vertical profile of (a) the meridional wind at San Cristobal and (b) the zonal wind over Managua. Open circles and gray triangles correspond to the dry-day means and the solid dots and triangles correspond to the wet-day means.

independent wind field composites. Figures 15a and 15b show the wet minus dry composite of the horizontal wind field, averaged over the 1000–850-hPa layer for the rainy season of 1997 and for the rainy seasons of 1990–94, respectively. Both figures clearly show the westerly flow anomaly in the eastern Pacific, the southerly component of the flow across the equator, the weakening of the western Caribbean trade winds, and the centers of cyclonic shear of the flow anomaly over southwestern Mexico and Gulf of Mexico. To determine whether the cyclonic anomaly in the eastern Pacific southwest of Mexico in the 1997 composite is a result of a single, strong event, rather than a frequent feature of the wind flow, each of the days composing the 1997 composite at 850 hPa were analyzed. Ten out of 18 wet spells over Central America coincided with a cyclonic vortex centered just off the southwestern coast of Mexico and 12 out of 13 dry spells coincided with an anticyclonic shear in the same region. The smaller number
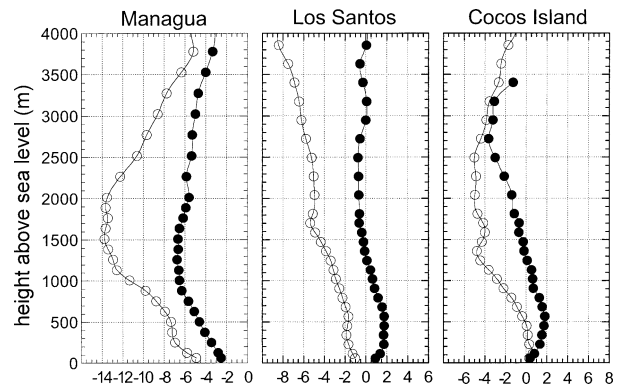


FIG. 13. Vertical profiles of the zonal wind (m s$^{-1}$) at Managua, Los Santos, and Cocos Island during wet (solid) and dry (open) spells.
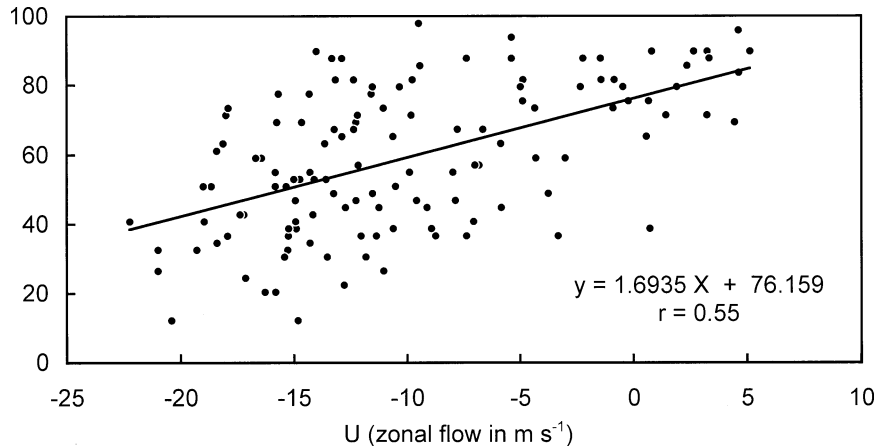
FIG. 14. Scatterplot of the percentage of stations reporting rainfall as a function of the intensity of the 1512-m (~850 hPa) zonal wind at Managua during May–Oct 1997.

of wet/dry spells in the 1997 composite results in a greater sensitivity to individual events. This is the case with the large wind anomalies over the northeastern and southeastern Pacific that appear in the 1997 composite, but not in the 1990–94 composite.

Figures 16a and 16b show the composites for 1997 and 1990–94 of the vertically averaged wind field in the 500–700-hPa layer. Both composites show westerly flow anomalies from 5°S to 15°N in the eastern Pacific with associated cyclonic shear centers located just southwest of Mexico and over the western Gulf of Mexico. Although the westerly flow anomaly is prominent over the Caribbean Sea in 1997 it is absent in the 1990–94 composite, indicating the lack of correlation of the strength of easterly trade winds in this layer with the wet and dry spell variations.

### b. OLR and moisture composites

OLR composites were made to assess the geographical extension of wet and dry spells. The composites of the wet minus dry spell differences for both the 1990–94 and 1997 rainy seasons are shown in Fig. 17. Both composites show a maximum variation just off the Pacific coast of Costa Rica. This similarity demonstrates that, despite strong interannual variations in the number of wet and dry spells, the main patterns of spatial variability remain. How large these differences are with respect to the mean and how the pattern associated with wet and dry spells evolves is investigated by computing the mean OLR of the six rainy seasons and the departures with respect to this mean. The 6-yr seasonal mean OLR and the standard deviation with respect to this mean are shown in Fig. 18. The largest values of the mean OLR, corresponding to either low clouds or cloudless regions, are located over extratropical regions, while the lowest values are located between 5° and 10°N, associated with the ITCZ. The maximum standard deviation is located over the Pacific Ocean, southwest of

Mexico, but north of the ITCZ. This coincides with the region of tropical cyclone formation in the eastern Pacific. The region of higher variability extends northward over western Mexico into the Mexican monsoon region (Douglas et al. 1993).

The OLR anomaly composite for the wettest days (Fig. 19a) shows negative values, suggesting an extended area of deep convection, well into the eastern Pacific and just off the south coast of Mexico and the Pacific coast of northern Central America. The location of the maximum negative anomaly in the wet composite occurs over the ocean rather than over land, suggesting either that cold cloudiness is more frequent offshore during wet spells, possibly a result of more frequent land-breeze-induced convection, more frequent tropical depression/storm formation, or that prevailing northeasterly winds in the upper troposphere advect clouds from over the land to the region offshore. Quite possibly all three factors contribute to the offshore maximum. The region of negative anomalies also extends over the far western Caribbean Sea. Another feature of the wet composite is the suppression of cloudiness (positive anomaly) in the region just north of the equator and west of 100°W. This band of positive anomaly in OLR, taken together with the negative anomaly band in OLR found just south of the coast of southern Mexico and Central America, might be interpreted as the result of a northward movement of the ITCZ.

The OLR anomaly composite for the driest days (Fig. 19b) shows the largest positive values, or less deep and/or less frequent convection, centered south of Panama and over northwestern Colombia. The positive anomaly extends westward over the eastern Pacific in a band centered at 5°N, and eastward across northern South America. It is curious that enhanced convection (negative OLR) is indicated southwest of Mexico, over the Pacific, though this is less than the OLR anomaly during the wettest days. The reasons for this are unclear.

Composites of the specific humidity and moisture
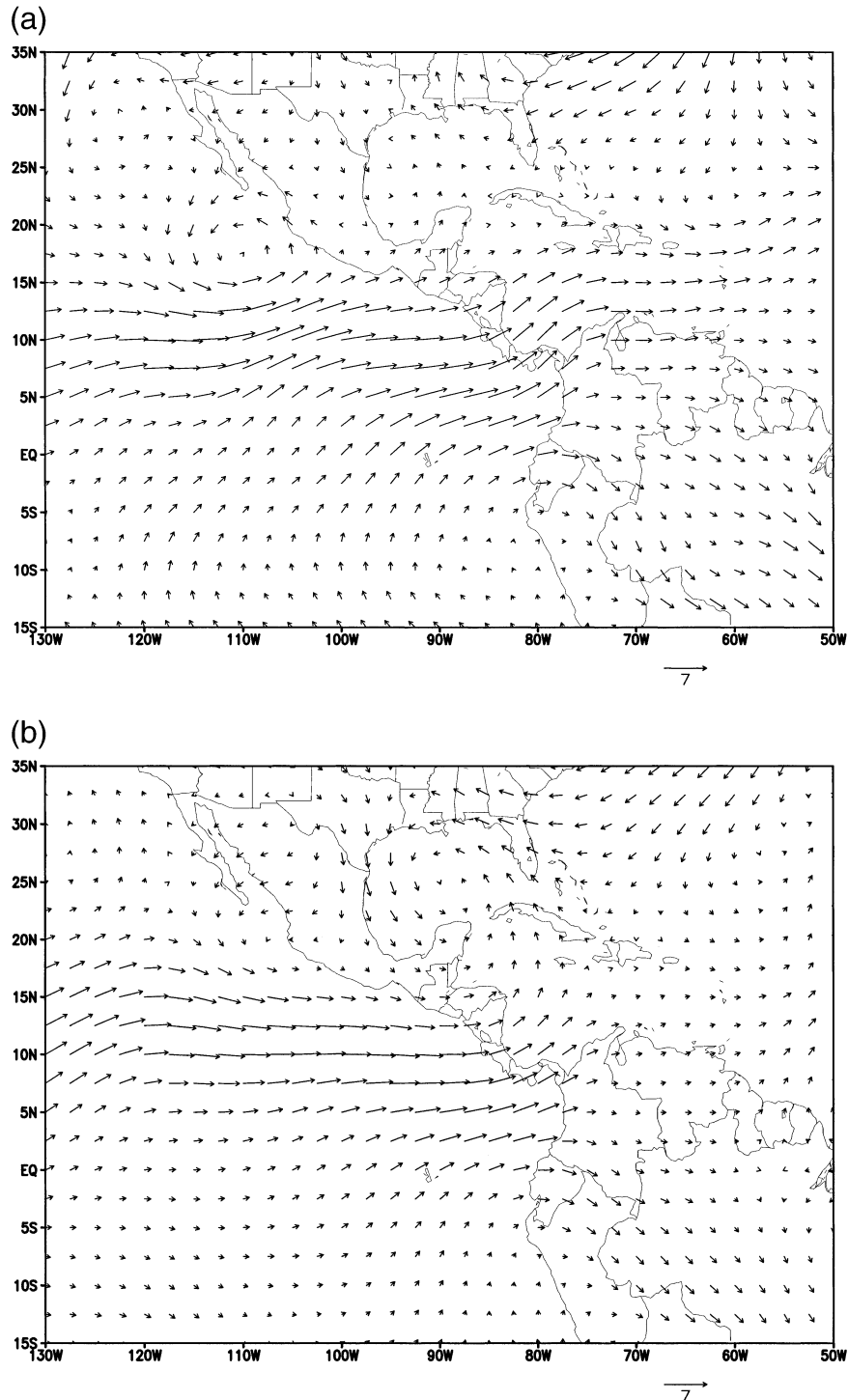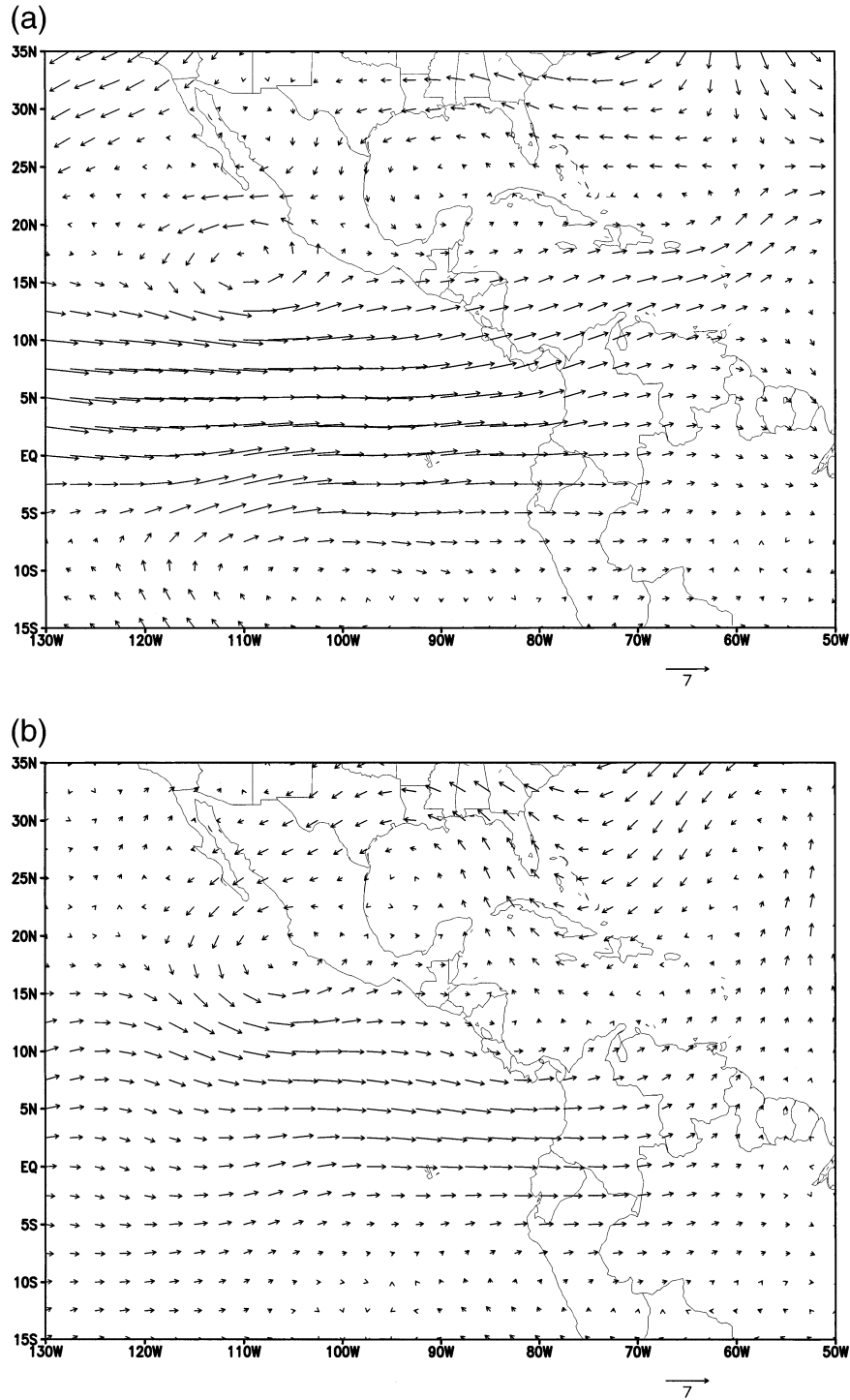
(a)



(b)



FIG. 15. Horizontal wind field of the wet minus dry days, averaged over the 1000–850-hPa layer, for the rainy seasons of (a) 1997 and (b) 1990–94. Vector at bottom in m s$^{-1}$.

convergence were made from the NCEP reanalysis data to complement the picture of wet and dry spells. In the equatorial region the large-scale humidity field varies very little compared with the extratropics. Typical standard deviations of specific humidity over Central Amer-

ica and surrounding oceans are less than 0.8 g kg$^{-1}$ at 1000 hPa and remain below 1.0 g kg$^{-1}$ in the lower troposphere. In Fig. 20, the vertical profile of the specific humidity anomaly with respect to the wet season climatological values is presented for reanalysis grid points

(a)



(b)



FIG. 16. Horizontal wind field of the wet minus dry days, averaged over the 700–500-hPa layer, for the rainy seasons of (a) 1997 and (b) 1990–94. Vector at bottom in m s$^{-1}$.

located over the western Caribbean Sea, just south of Costa Rica, and near San Cristobal, respectively. Over the western Caribbean Sea (Fig. 20a) the specific humidity profile during wet and dry spells is similar in the boundary layer but at midtropospheric levels it is clearly drier during dry spells and wetter during wet spells. Figure 20b shows the vertical profile at a grid point located in the maximum OLR anomaly of the wet minus dry composite (Fig. 17b). Here positive/negative anomalies of the specific humidity occur during the wet/

(a)



(b)
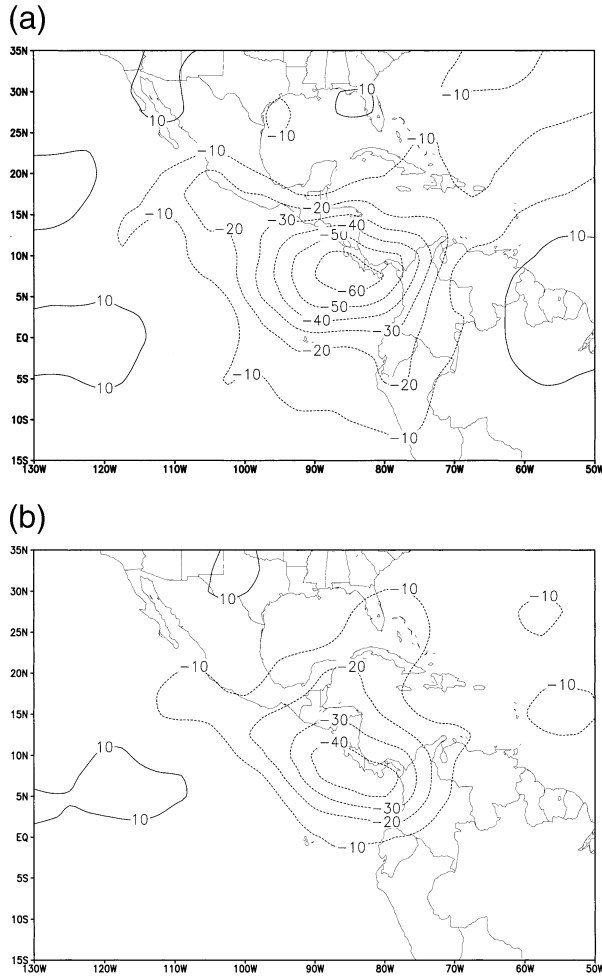


FIG. 17. OLR difference composite of wet and dry spells during the rainy season of (a) 1997 and (b) 1990–94. Contours are every 10 W m$^{-2}$, with negative contours dashed.

dry spells up through the 500-hPa level. In both the Caribbean Sea and near OLR maximum locations the humidity variation is greater at higher levels than near the surface (this is especially true of the relative humidity). The increase in humidity at midtropospheric levels is usually ascribed to the effect of the enhanced convective activity.

Near San Cristobal (Fig. 20c) the dry spell composite is more humid than the wet spell composite. Because San Cristobal is always located well south of the ITCZ during the May–October period, wet spells over Central America do not correspond to higher specific humidity there. On the contrary, higher specific humidities over San Cristobal may imply that the location of the ITCZ is displaced more to the south than normal—a condition with less rainfall in Central America. In addition, during wet spells the meridional winds at San Cristobal are stronger than normal (Fig. 9), which may result in slightly cooler, drier conditions compared with weaker meridional flow conditions.
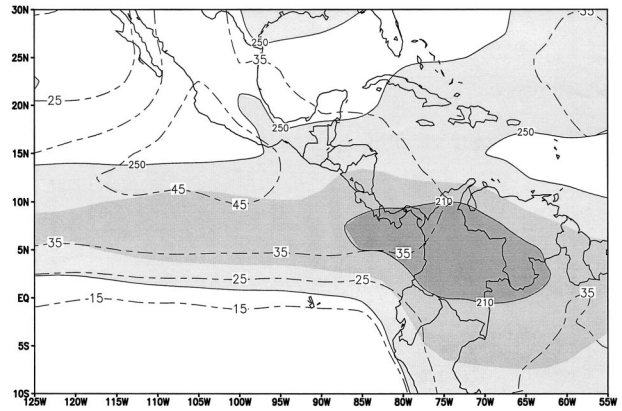


FIG. 18. OLR average (solid contours) and standard deviation (dotted contours) of the six (1990–94, and 1997) rainy seasons. Units are W m$^{-2}$.

Figure 20 shows that the difference in humidity between wet and dry spells is not large in an absolute sense; the dry minus wet difference at 850 hPa at the point south of Costa Rica, about 0.6 g kg$^{-1}$, is only
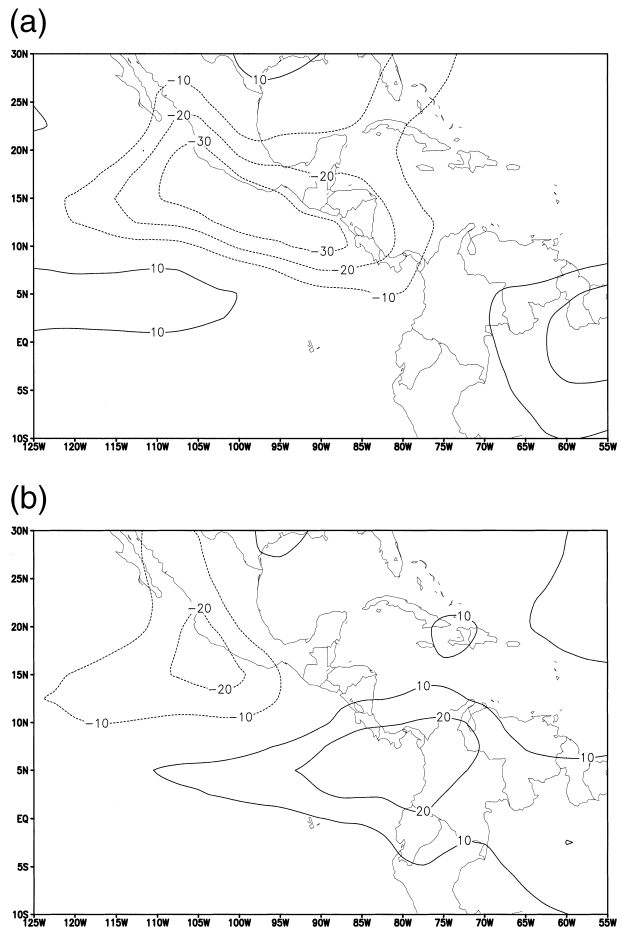
(a)



(b)



FIG. 19. OLR anomaly composite for (a) the wettest and (b) the driest days for the six (1990–94, and 1997) rainy seasons.
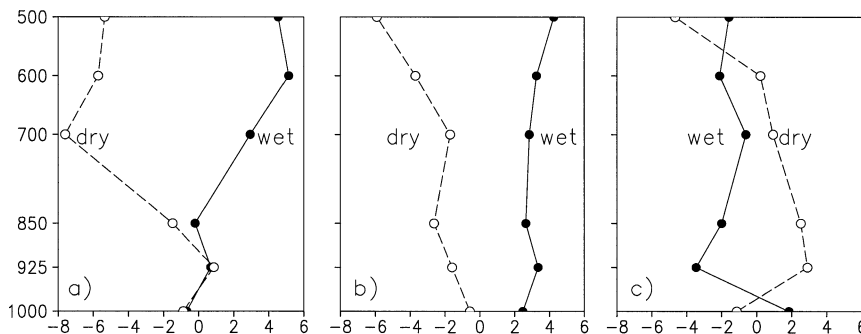
FIG. 20. Vertical profile of specific humidity anomaly (from NCEP reanalysis data) near (a) the western Caribbean Sea (12.5°N, 80°W), (b) south of Costa Rica (7.5°N, 82.5°W), and (c) San Cristobal (0°, 90°W) for the rainy season of 1997. Anomalies are computed with respect to the 1997 rainy season. Solid line corresponds to wet and dashed line to dry spell composites. Units are in tenths of g kg$^{-1}$. Pressure (hPa) is along the vertical axis.

about 4% of the saturated value (~16 g kg$^{-1}$, estimated using mean wet season conditions). This indicates that variations in moisture fluxes are dominated by the wind variations, which, between wet and dry spells, show much larger percentage variations (see Figs. 10, 12).

Figure 21 shows the difference between the wet composite and the dry composite of the reanalysis moisture convergence fields at 925 hPa, which is the level with the strongest signal. The figure indicates divergence of moisture in a band from 5°S to 5°N over the eastern Pacific and a band of convergence over Central America, extending westward to a maximum near 15°N, 110°W. This pattern, though somewhat noisy, roughly agrees with the OLR anomaly for the wet composite (Fig. 19a). The enhanced 925-hPa divergence in the near-equatorial region during wet spells, suggesting greater than average subsidence in the lower troposphere, is consistent with the humidity profile for the San Cristobal location (Fig. 20c), which was drier during wet spells. The other sites whose humidity profiles are shown in Fig. 20 fall within the region of enhanced 925-hPa convergence during wet spells evident in Fig. 21.

## 6. Summary and concluding remarks

This study has shown the feasibility of using data from an enhanced upper-air network (pilot balloon data from the PACS-SONET project in conjunction with the conventional radiosonde network) to describe large-scale circulation patterns associated with synoptic time-scale dry and wet spells over Central America. The current research has benefited from special datasets from the region, including upper-air wind observations and daily rainfall observations. However, this study's wind field analyses were limited by modest sample size, which included only the wet and dry spells that occurred during the May–October period of 1997, and especially by the small number of wind observations above 500 hPa. The NCEP reanalyses were used to extend the study to the 1990–94 period and the decision to include the humidity field was based on the general agreement with the wind observations of the 1997 data. Wet and dry spells, determined by analyzing daily rainfall data from the Pacific side of Central America, are associated with variations in the large-scale flow over both the Caribbean Sea and the eastern tropical Pacific. Composite wind field anomalies generated from the NCEP reanalysis data agree reasonably well with composites made using the observations from the sounding network over the Caribbean and Central America. However, over the far eastern Pacific Ocean, a region typically devoid of routine observations, there are clear differences between analyses produced using the sounding data and those from the reanalysis data. Finally, compositing techniques, applied to OLR and reanalysis-calculated moisture fields, have been useful for displaying the spatial extent of the rainfall and possible mechanisms associated with wet and dry spells. In summary, the charac-
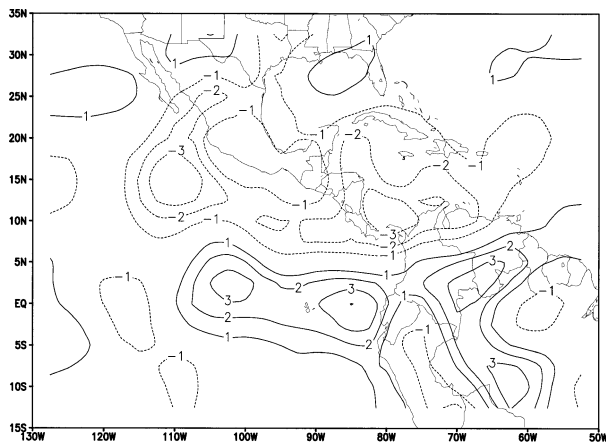


FIG. 21. Composite of the difference wet minus dry of the moisture convergence fields at 925 hPa for the rainy season of 1997. Dashed contours are negative (convergence); solid contours are positive (divergence). Units are 10$^{-5}$ s$^{-1}$.

teristics of summer season (May–October) Central American wet and dry spells found are as follows.

- Wet and dry spells on the Pacific side of Central America have a typical timescale of a few days with a recurrence period of about a week. Wet spells occur more often during the months of June and September–October. Dry spells during the rainy season occur more often during the month of July.
- Wet spells are associated with a midtropospheric cyclonic circulation anomaly over the western Caribbean Sea, weak trade winds throughout the lower troposphere across the Caribbean Sea and Central America, and relatively strong and deep cross-equatorial flow over the eastern Pacific. Dry spells coincide with a 500-hPa anticyclonic circulation anomaly over the western Caribbean Sea, strong trade wind flow over Central America, and weak and shallow cross-equatorial flow.
- Anomalies in the OLR fields associated with wet and dry spells extend well into the eastern Pacific. The largest differences in the OLR field between wet and dry spells occurs just south of Costa Rica, though the differences extend well into the eastern Pacific and over Central America and the far western Caribbean.
- While the number of wet and dry spells varies from year to year, the composites from two independent populations (rainy season of 1997 and rainy seasons of 1990–94) gave very similar results, indicating that the main synoptic features seen during the 1997 PACS-SONET observational period are representative of the longer-term conditions.

Our work during this study has raised questions that might benefit from further investigation. These observations and associated questions include the following.

- Wet and dry spells fluctuations seem to be modulated by lower-frequency variations. What are the processes involved in this intraseasonal variation?
- Dry spells on the Pacific slope of Central America are associated with stronger trade wind flow. This suggests that downslope wind effects are responsible for the decrease in rainfall on the Pacific side of Central America. Infrared satellite composites, on the other hand, show that the region of cold cloud suppression has a broader extension that includes not only the eastern Pacific but also some portions of the far western Caribbean. This suggests that a strengthening of the trade wind inversion, or some other process that reduces deep convection is occurring as well. Which mechanisms are responsible for the reduction in widespread convection?
- Although the fluctuations that this study focused on have timescales of more than a day, many of the rainfall forcing mechanisms during wet and dry spells are likely controlled by the diurnal cycle. How important is the synoptic-scale modulation of the diurnally driven local circulations such as sea breezes, and how does this affect the rainfall during wet and dry periods?
- The lack of agreement between the NCEP reanalyses and observations is largest in the near-equatorial eastern Pacific, and particularly at 700 hPa. Are these differences between the observations and the NCEP reanalysis due to the lack of observations in this region or is there a systematic error in the assimilating model's ability to reproduce the meridional circulation in this equatorial region?

## REFERENCES

Aberson, S. D., 1998: Five-day tropical cyclone track forecasts in the north Atlantic basin. *Wea. Forecasting,* **13,** 1005–1015.

Arkin, P. A., and B. N. Meisner, 1987: The relationship between large-scale convective rainfall and cold cloud over the Western Hemisphere during 1982–84. *Mon. Wea. Rev.,* **115,** 51–74.

Avila, L. A., and R. J. Pasch, 1992: Atlantic tropical systems of 1991. *Mon. Wea. Rev.,* **120,** 2688–2696.

——, and ——, 1995: Atlantic tropical systems of 1993. *Mon. Wea. Rev.,* **123,** 887–896.

——, and M. Mayfield, 1995: Eastern North Pacific hurricane season of 1993. *Mon. Wea. Rev.,* **123,** 897–906.

Bell, G. D., and Coauthors, 1999: Climate assessment for 1998. *Bull. Amer. Meteor. Soc.,* **80,** S1–S48.

Douglas, M. W., 1991: Cost-effective upper wind observing networks for developing countries. The SWAMP example. Preprints, *Lower Tropospheric Profiling: Needs and Technologies,* Boulder, CO, NCAR, NOAA Wave Propagation Lab., Amer. Meteor. Soc., German Meteor. Soc., and COST-74, 115–116.

——, and W. Fernández, 1997: Strengthening the meteorological sounding network over the tropical eastern Pacific Ocean and the intertropical Americas. *WMO Bulletin,* **46** (4), 348–351.

——, R. A. Maddox, K. Howard, and S. Reyes, 1993: The Mexican monsoon. *J. Climate,* **6,** 1665–1677.

Estoque, M. A., 1962: The sea breeze as a function of the prevailing synoptic situation. *J. Atmos. Sci.,* **19,** 244–250.

Fernández, W., and J. A. Barrantes, 1996: The Central American temporal: A long-lived tropical rain-producing system. *Top. Meteor. Oceanogr.,* **3** (2), 73–88.

——, and N. Vega, 1996: A comparative study of hurricanes Fifi (1974) and Greta (1978) and their associated rainfall distribution over Central America. *Top. Meteor. Oceanogr.,* **3** (2), 89–106.

Frank, N. L., 1976: Atlantic tropical systems of 1975. *Mon. Wea. Rev.,* **104,** 466–474.

Galo, E. R., W. Fernández, and E. Zarate, 1996: Aspectos sinópticos y dinámicos del temporal del 29 de Octubre al 3 de Noviembre de 1985 sobre Costa Rica. *Top. Meteor. Oceanogr.,* **3** (2), 107–123.

Garreaud, R. D., and J. M. Wallace, 1997: The diurnal march of convective cloudiness over the Americas. *Mon. Wea. Rev.,* **125,** 3157–3171.

Gruber, A., and J. S. Winston, 1978: Earth–atmosphere radiative heating based on NOAA scanning radiometer measurements. *Bull. Amer. Meteor. Soc.,* **59,** 1570–1573.

——, and A. F. Krueger, 1984: The status of the NOAA outgoing longwave radiation data set. *Bull. Amer. Meteor. Soc.,* **65,** 958–962.

Hastenrath, S., 1967: Rainfall distribution and regime in Central America. *Arch. Meteor. Geophys. Bioklimatol.,* **15B,** 201–241.

——, 1985: *Climate and Circulation of the Tropics.* D. Reidel, 455 pp.

Hellin, J., H. Haigh, and F. Marks, 1999: Rainfall charateristics of Hurricane Mitch. *Nature,* **399,** 316–316.

Kalnay, E., and Coauthors, 1996: The NCEP/NCAR 40-Year Reanalysis Project. *Bull. Amer. Meteor. Soc.,* **77,** 437–471.

Lawrence, M. B., and E. N. Rappaport, 1994: Eastern North Pacific hurricane season of 1992. *Mon. Wea. Rev.,* **122,** 549–558.

Lessmann, H., 1964: Synoptic and climatologic views on the rainfall in Central America, especially in El Salvador. *Proc. Symp. on Tropical Meteorology,* Wellington, New Zealand, New Zealand Meteorological Service, 295–305.

Liebmann, B., and C. A. Smith, 1996: Description of a complete (interpolated) outgoing longwave radiation dataset. *Bull. Amer. Meteor. Soc.,* **77,** 1275–1277.

Magaña, V., J. Amador, and S. Medina, 1999: The midsummer drought over Mexico and Central America. *J. Climate,* **12,** 1577–1588.

Nieto Ferreira, R., and W. H. Schubert, 1997: Barotropic aspects of ITCZ breakdown. *J. Atmos. Sci.,* **54,** 261–285.

Pallmann, A. J., 1968a: The synoptics, dynamics and energetics of the temporal using satellite radiation data (in addition to conventional observations). Second Year's Rep. 1, Department of Geophysics, Saint Louis University, St. Louis, MO (prepared for National Satellite Center, Environmental Science Services Administration).

——, 1968b: The synoptics, dynamics and energetics of the temporal using satellite radiation data (in addition to conventional observations). Second Year's Rep. 2, Department of Geophysics, Saint Louis University, St. Louis, MO (prepared for National Satellite Center, Environmental Science Services Administration), 16 pp. plus figures.

——, and C. J. Murino, 1967: The synoptics, dynamics and energetics of the temporal using satellite radiation data. First Year's Final Rep. Department of Geophysics, Saint Louis University, St. Louis, MO (prepared for National Satellite Center, Environmental Science Services Administration).

Pasch, R. J., and M. Mayfield, 1996: Eastern North Pacific hurricane season of 1994. *Mon. Wea. Rev.,* **124,** 1579–1590.

——, L. A. Avila, and J. Jiing, 1998: Atlantic tropical systems of 1994 and 1995: A comparison of a quiet season to a near-record-breaking one. *Mon. Wea. Rev.,* **126,** 1106–1123.

Portig, W., 1958: Der Temporal von ende oktober 1957. *Meteor. Rundsch.,* **11,** 150–156.

——, 1976: The climate of Central America. *Climates of Central and South America,* W. Schwerdtfeger, Ed., World Survey of Climatology, Vol. 12, Elsevier, 405–478.

Ramage, C. S., 1971: *Monsoon Meteorology.* J. van Mieghem, Ed., International Geophysics Series, Vol. 15, Academic Press, 296 pp.

Rappaport, E. N., and M. Mayfield, 1992: Eastern North Pacific hurricane season of 1991. *Mon. Wea. Rev.,* **120,** 2697–2708.

Riehl, H., 1979: *Climate and Weather in the Tropics.* Academic Press, 611 pp.

Sadler, J. C., M. A. Lander, A. M. Hori, and L. K. Oda, 1987: *Pacific Ocean.* Vol. II. *Tropical Marine Climatic Atlas,* Tropical Ocean and Atmosphere and Equatorial Pacific Ocean Climate Studies, Department of Meteorology, University of Hawaii, 27 pp.

Wang, J., and P. W. Leftwich, 1984: A major low-level cross-equatorial current at 110°E during the northern summer and its relation to typhoon activities. *Sci. Atmos. Sin.,* **8,** 443–449.

Xie, P., and P. A. Arkin, 1998: Global monthly precipitation estimates from satellite-observed outgoing longwave radiation. *J. Climate,* **11,** 137–164.